IRIS AperTO

UNIVERSITÀ DEGLI STUDI DI TORINO

AperTO - Archivio Istituzionale Open Access dell'Università di Torino

Testing ecological interactions between Gnomoniopsis castaneae and Dryocosmus kuriphilus

This is the author's manuscript

Original Citation:

Availability:

This version is available http://hdl.handle.net/2318/1607357 since 2017-05-25T16:27:08Z

Published version:

DOI:10.1016/j.actao.2016.08.008

Terms of use:

Open Access

Anyone can freely access the full text of works made available as "Open Access". Works made available under a Creative Commons license can be used according to the terms and conditions of said license. Use of all other works requires consent of the right holder (author or publisher) if not exempted from copyright protection by the applicable law.

(Article begins on next page)

28 April 2024

UNIVERSITÀ DEGLI STUDI DI TORINO

***This is an author version of the contribution**:*
Questa è la versione dell'autore dell'opera:
[Lione G., Giordano L., Ferracini C., Alma A., Gonthier P., 2016. Acta Oecologica, 77, pp. 10-17, DOI: 10.1016/j.actao.2016.08.008]

]

The definitive version is available at:
La versione definitiva è disponibile alla URL:
[http://www.sciencedirect.com/science/article/pii/S1146609X16301813]

Testing ecological interactions between *Gnomoniopsis castaneae* and *Dryocosmus kuriphilus*

Guglielmo Lione[a], Luana Giordano[a,b], Chiara Ferracini[a], Alberto Alma[a] and Paolo Gonthier[a]

[a] Department of Agricultural, Forest and Food Sciences, University of Torino, Largo Paolo Braccini 2, 10095 Grugliasco, Italy

[b] Centre of Competence for the Innovation in the Agro-Environmental Field (AGROINNOVA), University of Torino, Largo Paolo Braccini 2, 10095 Grugliasco, Italy

Corresponding author: Paolo Gonthier (paolo.gonthier@unito.it)

Role of Authors

GL and LG conducted samplings and fungal isolations. GL performed statistical analyses and LG molecular diagnostics assays. GL and PG designed the experiments and wrote the manuscript. CF helped with the manipulation of insects and with the interpretation of results. AA supervised the work on insects and revised the manuscript.

Abstract

An emerging nut rot of chestnut caused by the fungus *Gnomoniopsis castaneae* was reported soon after the invasion of the exotic gall wasp *Dryocosmus kuriphilus* in Italy. The goal of this work was to assess the association between the spread of the fungal pathogen and the infestation of the pest by testing if:

I) viable inoculum of *G. castaneae* can be carried by adults of *D. kuriphilus*;

II) the fungal colonization is related to the number of adults inhabiting the galls;

III) the fungal colonization of chestnut buds and the oviposition are associated.

Fungal isolations and PCR-based molecular assays were performed on 323 chestnut galls and on their emerging *D. kuriphilus* adults, whose number was compared between galls colonized and not colonized by *G. castaneae*. To test the association between fungal colonization and oviposition, Monte Carlo simulations assuming different scenarios of ecological interactions were carried out and validated through isolation trials performed on 597 and 688 chestnut buds collected before and after oviposition, respectively.

Although DNA of *G. castaneae* was detected in a sample of 40% of the adults developed in colonized galls, the fungus could never be isolated from insects, suggesting that the pest is an unlikely vector of viable inoculum.

On average, the emerging adults were significantly more abundant from galls colonized by *G. castaneae* than from not colonized ones (3.76 *vs.* 2.54, $P<0.05$), indicating a possible fungus/pest synergy.

The simulations implying no interaction between *G. castaneae* and *D. kuriphilus* after fungal colonization were confirmed as the most likely. In fact, *G. castaneae* was present in 33.8% of the buds before oviposition, while no association was detected between fungal colonization and oviposition (odds ratio 0.98, 0.71-1.33 95% CI). This finding suggests that the fungus/pest synergy is asymmetrically favorable to the pest and occurs after oviposition.

Keywords: *Dryocosmus kuriphilus,* fungi, *Gnomoniopsis castaneae, Gnomoniopsis smithogilvyi,* insects, Monte Carlo

1. Introduction

Interspecific interactions stand among the major forces driving the ecosystem dynamics and resulting in effects which are perceptible at both structural and functional levels (Jones et al., 1994; Tilman, 1999). Interactions between plant pathogens and insects have been well-documented in agricultural and forest ecosystems as pivotal factors enhancing the occurrence, the transmission and the spread of plant diseases. Pathogenic fungi (Paine et al., 1997; Carlile et al., 2001; Harrington, 2013), bacteria (Harrison et al., 1980; Redak et al., 2004), phytoplasmas (Griffiths, 2013) and viruses (Spence, 2001) can be carried and released by insects through mechanical, metabolic, physiological, or trophic processes, depending on the case.

For some infectious diseases of trees, the ecological association relating fungal pathogens to insects has been identified as one of the main underlying features of the epidemiological processes. For instance, many fungal plant pathogens release volatile organic compounds that are highly attractive to some mycophagous insects. During the feeding process, the spores of the pathogen come into contact with the insects and can adhere on the surface of their exoskeleton, be collected in specialized anatomical structures or transported within the insect body. Subsequently, the contaminated insects may allow the fungal dispersal and transmit the pathogen from tree to tree, often through preexisting fresh wounds (Happ et al., 1971; Webber, 2004; Kirisits, 2013; Harrington, 2013).

The role played by the insects in the ecological association with fungal pathogens may extend beyond the transportation and the release of the spores. In fact, the vectors are often pests attacking the same host of the pathogen, leading to complex network of pest-pathogen-host interactions. For instance, pathogenic fungi requiring fresh wounds on the host tissues to start the infection process can be directly inoculated by their vectors during the excavation of galleries generated for feeding or breeding. While the fungal mycelium colonizes the host, the pests can take advantage of its presence either through the direct consumption of the fungus (i.e. mycophagia), or by feeding on an altered substrate with improved nutritional qualities (Paine et al., 1997). The synergy between the pathogen and the vector explains their mutual escalation, whose natural limitation relies in the increased death rate and in the alteration of the age structure occurring in the host trees population (Webber, 2004; Danti et al., 2013; Eckhardt, 2013; Kirisits, 2013).

Despite rarely documented, pests can also activate latent pathogens, whose switch from the endophytic to the pathogenic phase may be associated with the physiological reaction of the host to the pest attack (Sieber and Hugentobler, 1987).

The fungal-insect ecological interactions may explain the association between the spread of emerging pathogens and the biological invasion of exotic pests (Kirisits, 2013). Since 2005, a severe epidemic of nut rot has spread throughout the populations of the European chestnut (*Castanea sativa* Miller) in Italy, and its causal agent was described for the first time in 2012 as *Gnomoniopsis castaneae* G. Tamietti (syn: *G. smithogilvyi* L.A. Shuttlew., E.C.Y. Liew & D.I. Guest), an ascomycete included in the family of Gnomoniaceae (Visentin et al., 2012; Tamietti, 2016). *G. castaneae* is currently regarded as a major pathogen of chestnut in Italy, France and Switzerland (Visentin et al., 2012; Maresi et al., 2013; Dennert et al., 2015; Lione et al., 2015; Lione and Gonthier, 2016). Despite the pathogen lives as a parasite inside the kernel of the nut, it can also be isolated from the buds, the leaves, the bark of juvenile sprouts and from other green tissues of the tree where it does not induce any symptom. While fruiting bodies of the sexual form of *G. castaneae* can be observed on the burr surrounding the nut, the asexual stage of the fungus produces its multiplicative structures on the galls of *Dryocosmus kuriphilus* Yasumatsu (Visentin et al., 2012; Maresi et al., 2013). *D. kuriphilus*, commonly known as the Asian chestnut gall wasp, is a pest belonging to Hymenoptera Cynipidae that was accidentally introduced to Europe in the early 2000s (Quacchia et al., 2008). In the summer, *D. kuriphilus* lays eggs into the buds of chestnut, where its larvae overwinter. During the following vegetative season, the larvae develop within cells located in the inner tissues of the galls inducing

123 the formation of greenish-red galls, suppressing shoot elongation and causing twig
124 dieback (Ôtake, 1980). New adults emerge from the galls in the summer. A massive
125 presence of galls results in a dramatic reduction of the photosynthetic area, inhibits the
126 growth of the tree, decreases the chestnut vigor and determines substantial yield losses
127 (Kato and Hijii, 1997; EFSA, 2010; Sartor et al., 2015). Severe reduction of fruiting
128 estimated between 65% and 85% was observed in northern Italy, but recently the
129 presence of the pest has significantly decreased thanks to the biological control
130 programs performed with the Hymenoptera Torymidae *Torymus sinensis* Kamijo
131 (Ferracini et al., 2015).

132 Based on the first confirmed reports of the presence of *G. castaneae* and *D.*
133 *kuriphilus* in the European chestnut populations, the invasion of the pathogen occurred
134 a few years after the invasion of the pest and started in the same areas located in the
135 Cuneo Province, in north-western Italy (Brussino et al., 2002; Visentin et al., 2012),
136 suggesting that possible interactions between the pathogen and the pest may occur.
137 Although galls necrosis along with mortality of *D. kuriphilus* were observed in
138 association with *G. castaneae* (Magro et al., 2010), the ecological interaction between
139 the fungal pathogen and the exotic pest still remains widely unexplored.

140 The main goal of this work was to test some among the possible ecological
141 interactions between *G. castaneae* and *D. kuriphilus* by combining theoretical and
142 empirical approaches. In detail, three specific hypotheses of ecological interactions
143 were tested:

144 I) whether viable inoculum of *G. castaneae* can be carried by adults of *D. kuriphilus*;

II) whether the colonization of the gall tissues by *G. castaneae* is related to the number of inhabiting adults of *D. kuriphilus*;

III) whether the fungal colonization of plant buds and the oviposition by the insect are associated.

2. Methods

2.1. Experimental design

In each of the three sites located in north-western Italy (Table 1), five chestnuts were randomly selected. Branches with a maximum diameter of 1 cm harbored most *D. kuriphilus* galls and chestnut buds (see below), and thus were deemed to be representative for sampling purposes. From the crown of each tree, 10 branches were excised during two distinct samplings, the first one performed on 20th June 2013, before the oviposition timeframe of *D. kuriphilus*, while the second one was carried out on 25th September 2013, after the oviposition timeframe. The approximate starting date and the length of the oviposition timeframe were estimated according to EPPO (2005) and Alma et al. (2014).

2.2. Biological analyses

During the first sampling, 323 galls of *D. kuriphilus* were collected (up to two galls per branch, if present) and incubated separately into aerated plastic cages stored at

room temperature (~25±2 °C) and normal daylight exposure. The cages were visually inspected twice a day, for 3 weeks, and the 35% of the emerging adults of *D. kuriphilus* was plated into 6 cm diameter Petri dishes to isolate *G. castaneae* according to the protocol described in Giordano et al. (2013). The remaining adults were individually transferred using sterile tweezers into sterile 1.5 mL microcentrifuge tubes and stored at -20 °C. After 5 days without new emerging adults, the galls were removed from their incubator. In order to isolate *G. castaneae*, 5 fragments of approximately 5 × 5 × 1 mm were randomly excised from both the inner and the outer tissues of each gall and plated into 9 cm diameter Petri dishes filled with malt extract agar (MEA) (Visentin et al., 2012).

The isolation trials described above for the galls were performed on 597 and 688 buds (up to 5 buds per branch) after the first and the second sampling, respectively. A subset of 60 buds collected from the former sampling and all the buds obtained from the latter were sectioned under a dissecting microscope (20 × magnification) to assess the presence of *D. kuriphilus* eggs.

For both samplings, the identification of the pathogen was performed based on the macro and micro-morphological features of growing colonies, as described in Visentin et al. (2012) and Lione et al. (2015).

2.3. Molecular analyses

A subset of 40 insects, half emerged from galls colonized by *G. castaneae* and half from galls not colonized (see Results), was drawn from the adults of *D. kuriphilus* previously stored at -20 °C. On this subset, PCR-based molecular analyses were

191 performed to validate the results of the isolation trials (i.e. molecular validation). Fungal
192 DNA extraction was carried out by using the E.Z.N.A.™ Stool DNA Isolation Kit (Omega
193 Bio-Tek, Norcross, GA, USA) following the manufacturer's instructions. *G. castaneae*
194 was identified through a taxon-specific molecular diagnostic assay. The two primers
195 Gc1f (5'-AGCGGGCATGCCTGTTCGAG-3') and Gc1r (5'-
196 ACGGCAAGAGCAACCGCCAG-3') were used as described in Lione et al. (2015) to
197 specifically detect *G. castaneae*. All PCRs were carried out by setting the thermocycler
198 parameters as follows: an initial 95°C denaturation step of 5 min, followed by 35 cycles
199 of 95 °C denaturation for 30 s, 62 °C annealing for 45 s and 72 °C extension for 1 min,
200 and a final 72 °C extension step of 10 min. The specific amplicon of *G. castaneae* (168
201 bp) was visualized in gel containing 1% (w/v) of high resolution MetaPhor (Cambrex)
202 and 1% (w/v) of standard agarose, after electrophoretic migration. In order to assess the
203 efficiency of fungal DNA extraction, an additional PCR amplification of the Internal
204 Transcribed Spacer (ITS) was performed with the universal primers ITS1 and ITS4
205 (White et al., 1990; Gardes et al., 1991).
206 Moreover, the above cited taxon-specific molecular assay was carried out on a
207 random subset of 50 putative colonies of *G. castaneae* to confirm the morphological
208 identifications.
209
210 **2.4. Statistical analysis and Monte Carlo simulations**
211
212 According to the results of the isolation trial, the galls were classified as
213 colonized (GC^+) or not colonized (GC^-) by *G. castaneae*. Negative binomial generalized

linear regression models (nbGLM), parametrized with the intercept, were run to compare the average number of adults of *D. kuriphilus* emerged from GC^+ (codified as 1) and GC^- (codified as 0) (Venables and Ripley, 2002; Kéry, 2010). One nbGLM per site and an overall model for the three sites were fitted.

In both GC^+ and GC^-, the proportion (%) of *D. kuriphilus* adults positive to *G. castaneae* (A^+) was calculated separately for the isolation trial and for the molecular validation along with the exact 95% confidence intervals (95% CI) obtained as reported by Blaker (2000). The proportion of A^+ was compared between GC^+ and GC^- with the Fisher's exact test (Crawley, 2013).

A Monte Carlo (MC) experiment (Carsey and Harden, 2014) was set to test *in silico* the association between the colonization of *G. castaneae* and the oviposition by *D. kuriphilus*. An artificial environment was designed to simulate the oviposition and the fungal colonization processes at buds level. In a cubic Cartesian space with edges bounded between 0 and 40 cm, three branches of 35 cm, each one with three twigs of 5 cm were designed. A single branch included 20 buds, while 5 buds were located along each twig, achieving a total of 105 buds. The probability density functions (PDFs) of the distances separating two consecutive buds on the branches and on the twigs were estimated through the fit of the distribution types included in the Pearson system (Pearson, 1895; Lachene, 2013). The fit was performed on the pooled distances measured on four model branches and on their twigs collected in the field during the first sampling. The optimal Pearson type PDF was selected according to the minimum Akaike Information Criterion (AIC) (Akaike, 1973; Crawley, 2013). Two scenarios of asymmetric association (Somers, 1962) between fungal colonization and oviposition,

and between oviposition and fungal colonization were simulated: scenario A) the fungal colonization may influence the insect oviposition; scenario B) the insect oviposition may influence the fungal colonization. Each scenario was simulated under two competing hypotheses. In the scenario A, the hypothesis A_1 assumed that the buds colonized (BC^+) and not colonized (BC^-) by *G. castaneae* were equally attractive to *D. kuriphilus*, while under the alternative hypothesis A_2 the BC^+ were more likely to attract ovipositing insects than BC^-. Similarly, in the scenario B, the buds oviposited (BO^+) were as attractive to the fungus as the not oviposited ones (BO^-), under the hypothesis B_1, while BO^+ were more attractive to *G. castaneae* than BO^-, under the competing hypothesis B_2. For the scenario A, the attraction exerted by the buds was modelled as a series spherical buffers (Mitchell, 1999). Each spherical buffer was centered in the associated bud coordinates, while the radius was weighted differently according to the hypothesis being simulated. The radius was set constant at 0.5 cm for all the buds under A_1, while under A_2 it was set to 0.5 cm for BC^- and to 1 cm for BC^+. For the scenario B, the attraction was modeled as a numeric weight assigned to the buds. Under B_1 the weight was set to 0.5 in order to assign to all buds an even probability of extraction regardless of the oviposition status. The probability of extraction was automatically rescaled by the sampling algorithm based on random number generators (Mitchell, 2005; Carsey and Harden, 2014). Under B_2 the weight was tuned to 0.2 for BO^- and to 0.8 for BO^+ in order to simulate a different attraction, depending on the oviposition status, without introducing an asymmetry hyperparameter (i.e. different attractiveness weights were evenly spaced around the equal attractiveness weight) (Mitchell, 2005; Kéry, 2010; Carsey and Harden, 2014). The oviposition process of a single adult of *D. kuriphilus*

was simulated by modelling the insect trajectory as a Lévy flight. The Lévy flight was generated as a three dimensional random walk whose steps were derived from a power-law tailed PDF, with parameter a=1 and μ=2, and whose zenith and azimuth were drawn, at each step, from a uniform distribution bounded between 0 and 2π radians (Reynolds and Frye, 2007; Edwards, 2008; Kéry, 2010). The status BO^+ was assigned to the bud whose buffer included for the first time the ending point of a single step of the Lévy flight. The fungal colonization was modelled as a stochastic process, based on a random number generator, drawing buds and assigning to them the BC^+ status according to an extraction probability proportional to a weight (Carsey and Harden, 2014). The weight was attributed to the buds depending on the hypothesis being tested (see below). Within each hypothesis the ratio between BC^+ and the total buds (i.e. g) was set to g = 20%, 40%, 60%, 80%. Similarly, the number of adults was set as a proportion of the maximum number of buds that could be oviposited in percent, selecting for this percent (d) the same values attributed to g (i.e. d = 20%, 40%, 60%, 80%). Each combination between g and d and the additional combination g=50% and d=60% were set as a couple of fixed parameters to run a block of 5000 Monte Carlo (MC) simulations. Within each hypothesis, 17 blocks of MC simulation were run, for a total of $3.4 \cdot 10^5$ simulations (2 scenarios · 2 hypotheses · 17 blocks · 5000 simulations). In the scenario A, each MC simulation consisted in the following steps: 1) drawing the g BC^+ after the fungal colonization process was run with a weight set constant for all the 105 buds; 2) running d independent oviposition processes of a single adult of *D. kuriphilus* to gather BO^+, with the radii of the spherical buffers set as described above for each hypothesis; 3) cross-tabulating the BC^+, BC^-, BO^+ and BO^- and calculating the

odds ratio θ as the measure of association between fungal colonization and oviposition (Agresti, 2001). Every MC simulation in the scenario B was performed through the following steps: 1) retrieving the BO^+ from A_1, step 2; 2) running the fungal colonization process with the weights assigned to BO^+ and BO^-, depending on the buds attraction tuned according to hypotheses described above, and drawing the g BC^+; 3-4) replicating previous steps 3 and 4. The 5000 θ values obtained within the blocks were used to estimate the PDFs of the odds ratios, whose average $\bar{\theta}$ was calculated with its 95% CI lower and upper bounds (i.e. $\bar{\theta}_l$ and $\bar{\theta}_u$) (Buckland, 1983; Jones et al., 2009). MC algorithms were run in R 3.2.1. (scripts are available as Supplementary Material Appendix A).

The MC simulations were biologically validated with the results gathered during the isolation trials performed on the buds. For both samplings, the ratio g_o between BC^+ and the total buds was calculated with its 95% CI (Blaker, 2000) separately for each site and conjointly for all sites. The g_o values were compared between the two samplings with the Fisher's exact test. For the second sampling, the ratio d_o between BO^+ and the total buds was calculated as described for g_o. The fungal colonization and the oviposition status of the buds were cross-tabulated and the odds ratio θ_o with its 95% CI (i.e. θ_{ol} and θ_{ou}) were calculated with the Fisher's method. Subsequently, θ_o, θ_{ol} and θ_{ou} were compared to the average odds ratios and their associated 95% CI obtained from the MC simulations (Agresti, 2001; Carsey and Harden, 2014). The comparison was performed by assessing the probability (L) of gathering *in silico* an outcome statistically equivalent to the values obtained through the field samplings and the laboratory analyses, conditional to the occurrence of each hypothesis (i.e. the likelihood of θ_o, θ_{ol}

306 and θ_{ou}). L was calculated within the hypotheses as the relative frequency of MC
307 simulation blocks whose θ, θ_l and θ_u were statistically equivalent to θ_o, θ_{ol} and θ_{ou} (i.e.
308 $L = \frac{\sum I(\theta_l<1<\theta_u)}{17}$ if $\theta_{ol} < 1 < \theta_{ou}$, $L = \frac{\sum I(\theta_l>1)}{17}$ if $\theta_{ol} > 1$, otherwise $L = \frac{\sum I(0<\theta_u<1)}{17}$, where I is
309 the indicator function according to Iverson's notation) (Gerber et al., 2003; Kéry, 2010;
310 Carsey and Harden, 2014).
311 A threshold of 0.05 was set as cut-off for the rejection of the null hypotheses of
312 all statistical tests.
313

314 ## 3. Results

315
316 The taxon-specific molecular assay confirmed the morphological identifications of
317 all the putative colonies of *G. castaneae* tested. The isolation trial performed on the
318 galls resulted in 120 GC^+ and 203 GC^-, with a ratio between GC^+ and total number of
319 galls ranging from 16.0% to 67.7%, depending on the site. A total of 966 adults of *D.*
320 *kuriphilus* emerged from the galls, 451 from GC^+ and 515 from GC^-. On average, the
321 insects from GC^+ were significantly more abundant than the ones emerged from GC^-
322 (2.62-3.90 *vs.* 0.62-2.89, $P<0.05$), as shown by the P-values displayed by the β
323 coefficients in all the nbGLM (Table 2).
324 On the subset of adults scored for the presence of *G. castaneae*, 180 emerged
325 from GC^+ and 159 from GC^-. The proportion of A^+ assessed through the isolation trial
326 was 0% both for *D. kuriphilus* adults emerged from GC^+ (0-2.0% 95% CI) and for adults
327 deriving from GC^- (0-2.2% 95% CI), resulting in a not significant Fisher's exact test
328 ($P>0.05$). On the contrary, the proportion of A^+ determined through the molecular assay

329 raised to 40.0% (20.9-63.1% 95% CI) for the adults from GC^+, remaining stable at 0%
330 (0-16.0% 95% CI) for the others. The former proportion resulted significantly larger than
331 the latter ($P<0.05$).

332 The optimal fits for the PDFs of the distances separating two consecutive buds
333 corresponded to Pearson type III curves with shape, location and scale parameters of
334 1.89, 2.07 and 12.6 for the branches (AIC=435.3), and 2.20, -0.16, 5.72 for the twigs
335 (AIC=182.1). Depending on the g-d combination, the blocks of MC simulations
336 displayed mean values $\bar{\theta}$ of odds ratios ranging from 0.127 to 1.394 under the
337 hypothesis A_1, and $\bar{\theta}$ values comprised between 1.07 and 1.34 under the hypothesis
338 B_1. Under A_1, the 95% CI associated with $\bar{\theta}$ showed bounds comprised within the
339 ranges 0-0.46 for $\bar{\theta}_l$ and 1.47-5.46 for $\bar{\theta}_u$, while under B_1 the bounds ranged from 0.18
340 to 0.46 for $\bar{\theta}_l$ and from 2.14 to 5.68 for $\bar{\theta}_u$. No significant association between the
341 colonization of *G. castaneae* and the oviposition by *D. kuriphilus* emerged under both A_1
342 and B_1, since the value 1 was comprised between $\bar{\theta}_l$ and $\bar{\theta}_u$ in all blocks. Under the
343 alternative hypotheses, the corresponding g-d blocks of MC simulations displayed
344 ranges from 2.24 to 8.50 for $\bar{\theta}_l$, from 4.78 to 35.47 for $\bar{\theta}$ and from 6.25 to 102.5 for $\bar{\theta}_u$
345 in A_2, and from 1.60 to 5.44 for $\bar{\theta}_l$, from 5.74 to 21.86 for $\bar{\theta}$ and from 7.90 to 60.80 for
346 $\bar{\theta}_u$ in B_2. A positive and significant association between fungal colonization and the
347 oviposition arose, since the condition $1 \leq \bar{\theta}_l$ occurred in all blocks simulated under A_2
348 and B_2 (Table 3).

349 Depending on the site, the ratio g_o was comprised between 1.1% and 52.2%, and
350 between 30.7% and 48.5% in the first and in the second sampling, respectively,
351 displaying a significant increase only in the site of Aymavilles ($P<0.05$). The overall ratio

of g_o attained 33.8% in the first sampling and 40.7% in the second one, showing a significant raise between samplings ($P<0.05$) (Fig. 1). The subset of buds inspected for *D. kuriphilus* eggs showed the absence of oviposition in all buds collected during the first sampling. Instead, in the second sampling, the values displayed by the ratio d_o were 87.1% (82.0-91.2% 95% CI) in Aymavilles, 96.1% (92.8-98.2% 95% CI) in Nomaglio and 0% (0-1.6% 95% CI) in Robilante, with an overall value of 61.0% (57.3-64.7% 95% CI). The odds ratio θ_o obtained for the sites of Aymavilles (1.45, 0.59-3.58 95% CI), Nomaglio (0.75, 0.14-3.56 95% CI) as well as the overall value (0.98, 0.71-1.33 95% CI) were not significantly different from 1 ($P>0.05$). Instead, the corresponding value for Robilante could not be estimated since no oviposited buds were detected in the second sampling. The values of L were calculated according to the fact that the overall and within site 95% CI satisfied the condition $\theta_{ol} < 1 < \theta_{ou}$. In all cases, L attained the value 100% under A_1 and B_1, and 0% under the competing hypotheses.

4. Discussion

The spread of plant pathogens and the invasion of exotic pests may be closely associated, especially if they share the same hosts. Often, pathogen-pest ecological interactions have been proved to drive the spread of both the pathogen and the pest. Pathogens and pests can operate in synergy through a series of processes leading to mutual advantages, to the detriment of the host plant. In the case of fungal plant pathogens, pests can operate as vectors of viable inoculum, as agents responsible for the inoculation process and as constructors of micro-environments favorable to the

fungal colonization and reproduction. In return, the pathogen can alter the physical and the chemical qualities of the host tissues, providing the pests with an improved substrate for feeding and breeding. In some cases, the fungus may also represent a trophic resource for mycophagous insects (Paine et al., 1997; Webber, 2004; Danti et al., 2013; Eckhardt, 2013; Harrington, 2013; Kirisits, 2013).

The spatial and temporal overlaps between the outbreak of the nut rot of the European chestnut caused by *G. castaneae* and the biological invasion of *D. kuriphilus* occurring in Italy suggest a possible association between the emerging fungal pathogen and the exotic pest. The isolation trials indicate that *D. kuriphilus* is unlikely to carry viable inoculum of *G. castaneae*. In fact, if the pest was a vector, a certain amount of adults emerged from the colonized galls (GC^+) should have resulted positive to *G. castaneae*. Instead, the fungus was never isolated from the adults of *D. kuriphilus*, regardless of the presence or absence of viable inoculum colonizing the gall tissues. On the contrary, DNA of *G. castaneae* could be detected in a subset of the insects emerged from the colonized galls. These findings may indicate that, when *G. castaneae* colonizes the gall tissues, the emerging adults of *D. kuriphilus* are potentially able to carry a certain amount of inoculum. However, this inoculum is no longer viable and, consequently, it cannot contribute to the infection process and to the spread of the pathogen. Despite the separation between the putative inoculum present in the inner tissues of the insect body from the inoculum adhering on the exoskeleton was not performed, the isolation technique was suitable to reveal the presence of both, since the insects were mostly smashed during the plating process because of their structural fragility. However, since *D. kuriphilus* consumes part of the inner tissues of the galls, the

inoculum of *G. castaneae* in the form of mycelium might have been ingested and subsequently inactivated during the digestive processes, rather than transported on the surface of the exoskeleton. It should be noted that no specialized anatomical structures allowing fungal inoculum transportation are present on the exoskeleton of *D. kuriphilus*.

The significantly larger number of adults of *D. kuriphilus* hosted in the galls colonized by *G. castaneae* could be the result of an interaction occurring between the fungus and the pest during oviposition. *G. castaneae* colonizing the buds could exert an attractive effect towards the pest, yet also the oviposited buds could represent a more favorable environment for the fungal colonization. Testing these hypotheses *in silico* through Monte Carlo methods was advantageous, since such methods allowed to model and simulate iteratively the ecological phenomena (i.e. oviposition/colonization and attractiveness of oviposited/colonized buds) under different scenarios (i.e. influence of fungal colonization on oviposition, or influence of oviposition on fungal colonization) and with various combinations of biologically relevant parameters (i.e. number of adults and colonized buds). The oviposition by *D. kuriphilus* and the fungal colonization were modeled as stochastic processes based on Lévy flight and on random sampling from probability distributions, respectively. Despite the absence of studies specifically focused on *G. castaneae* and *D. kuriphilus*, these approaches have been proved to be effective and consistent with in-field observations when simulating the flight trajectory of insects and the dynamics of fungal colonization in several natural and semi-natural ecosystems (Reynolds and Frye, 2007; Edwards, 2008; Honkaniemi et al., 2014; Jarnevich and Young, 2015). Also the assignment of differential weights and the delimitation of buffers to model the buds attractiveness towards the fungus and the

421 insect were consistent with the methods proposed in the literature to investigate
422 ecological interactions (Mitchell, 1999; Mitchell, 2005; Gonthier et al., 2012). Regardless
423 of the scenario and of the number of adults and colonized buds, the outcomes of the
424 simulations (i.e. average odds ratios and associated 95% CI) showed that the
425 association between fungal colonization and oviposition by *D. kuriphilus* depends on
426 which hypothesis about the attraction exerted by the oviposited/colonized buds on the
427 fungus/pest is assumed. When modelling all the buds as equally attractive, no
428 ecological association between the two phenomena could be detected, meaning that no
429 interaction between *G. castaneae* and *D. kuriphilus* occurred. Conversely, when the
430 oviposited/colonized buds were modeled as more attractive to the fungus/pest,
431 significant and positive average odds ratios were displayed, indicating the existence of
432 an underlying interaction between *G. castaneae* and *D. kuriphilus*. The biological
433 validation is a pivotal step to carry out when testing hypotheses through MC simulations
434 (Thébaud et al., 2005). Even though the infection biology and epidemiology of *G.*
435 *castaneae*, with a few exceptions (Lione et al., 2015; Lione and Gonthier, 2016), are still
436 mostly unknown and, thus, no prior information is available to discriminate which
437 scenario is most likely to occur in nature, the option A seems to fit better to the
438 processes of fungal colonization and oviposition. Moreover, the probability of gathering
439 *in silico* outcomes statistically equivalent to the results gathered from the field trials
440 showed that the hypotheses of equal attractiveness exerted by all the buds towards the
441 fungus/insect are the most likely. These conclusions are supported by the fact that the
442 fungus was isolated from approximately 1/3 of the buds sampled prior to the oviposition
443 period, and also from the buds collected from the site where the oviposition was virtually

absent in both samplings. Despite the overall ratio of colonized buds showed a significant increase between the two samplings, the raise was not substantial (approximately +7%) and it was mostly influenced by the data gathered from one out of three sites. Considering that the incidence of *G. castaneae* has been shown to increase with warmer temperatures during the months preceding its assessment (Lione et al., 2015), and provided that in north-western Italy the warmest months of the year are comprised between the two sampling dates (Biancotti et al., 1998), the observed increase could depend on the climate, rather than on the oviposition by *D. kuriphilus*.

While the hypothesis of an ecological interaction between *G. castaneae* and *D. kuriphilus* during the oviposition stage is not supported, the larger number of adults inhabiting the galls colonized by the fungus suggests the possibility of an interaction occurring subsequently, during the insects development. The fungal mycelium could increase the survival rate of the pests by providing an additional nutritive source for direct consumption (i.e. mycophagy), or by improving the quality of the gall tissues through favorable chemical transformations. The mycelium of *G. castaneae* colonizing the galls might transform plant tissues into a more digestible biomass rich in nutrients. Despite no experimental results can be provided to support these hypotheses, the positive role of fungi on the diet and on the population dynamics of many insects has been largely documented in the literature (Kendrick, 2000; Carlile, 2001). The colonization of galls by *G. castaneae* may also result in a physical alteration of the plant tissues. Several fungi have been shown to induce changes in the firmness of substrates by softening their texture (Kendrick, 2000), which might result in a reduced mechanical resistance leading to an advantage to the insect. However, as noticed by Magro et al.

(2010), galls alteration might also be detrimental to *D. kuriphilus*. It is worth noting that since no necrosis or observable physicals alterations were observed on the galls colonized by *G. castaneae* in our study, the role of the fungus as inhibitor of *D. kuriphilus* that was suggested by Magro et al. (2010) would deserve further investigations. Moreover, specific studies are needed to clarify whether and how *G. castaneae* can modify the galls tissues.

5. Conclusion

The theoretical approach proposed and used in this study combined the results from different possible ecological interactions between *G. castaneae* and *D. kuriphilus*, while the biological analyses and the validation performed on field data allowed the detection of the most likely hypothesis. All lines of evidence suggest that the ecological interactions between *G. castaneae* and *D. kuriphilus* are asymmetrically favorable to the insect, rather than to the fungus. This is not surprising considering that the two species did not coevolve in their current area of sympatry. It is worth noting that, potentially, the infestations of *D. kuriphilus* could also have increased the spreading ability of the pathogen, since asexual fruiting bodies of *G. castaneae* have been observed on the galls surface (Maresi et al., 2013). However, asexual reproduction has been recently shown to play a minor role compared to sexual reproduction in the spread of the fungal pathogen based on population genetics data (Sillo et al., 2016). Moreover, as documented for other fungi (i.e. latent pathogens), the stress induced on the chestnut by a massive attack of the pest could increase the incidence of the disease (Petrini,

1991). Such observations suggest that the level of complexity in the ecological interaction between *G.castaneae* and *D. kuriphilus* might be influenced by other co-occurring factors. However, no studies on these topics are available yet and, to date, our results suggest that the diffusion of *G. castaneae* and the consequent outbreak of the nut rot of chestnut could have boosted the spread of the exotic pest in the newfound area of invasion in Italy.

Acknowledgements

This study was supported by a grant of Regione Piemonte through the activity of the "Chestnut Growing Center". The Authors wish to thank the anonymous Reviewers who, with their suggestions, contributed to the improvement of the paper.

References

Agresti, A., 2001. Exact inference for categorical data: recent advances and continuing controversies. Stat. Med. 20, 2709–2722.

Akaike, H., 1973. Information theory and an extension of the maximum likelihood principle, in: Petrov, B. N., Csaki, F. (Eds.), 2nd International Symposium on Information Theory, Akadémiai Kiadó, Budapest, pp. 267–281.

Alma, A., Ferracini, C., Saror, C., Ferrari, E., Botta, R., 2014. Il cinipide orientale del castagno: lotta biologica e sensibilità varietale. Italus Hortus 21, 15–29.

512 Biancotti, A., Bellardone, G., Bovo, S., Cagnazzi, B., Giacomelli, L., Marchisio, C., 1998.
513 Distribuzione Regionale di Piogge e Temperature, CIMA ICAM, Torino.

514 Blaker, H., 2000. Confidence curves and improved exact confidence intervals for
515 discrete distributions. The Can. J. Stat. 28, 793–798.

516 Brussino, G., Bosio, G., Baudino, M., Giordano, R., Ramello, F., Melika, G., 2002.
517 Pericoloso insetto esotico per il castagno europeo. L'Informatore Agrario 37, 59–61.

518 Buckland, S.T., 1983. Monte Carlo methods for confidence interval estimation using the
519 bootstrap technique. J. Appl. Stat. 10, 194–212.

520 Carlile, M.J., Watkinson, S.C., Gooday, G.W., 2001. The Fungi, second ed. Academic
521 Press, London.

522 Carsey, T.M., Harden, J.H., 2014. Monte Carlo Simulation and Resampling Methods for
523 Social Science, SAGE, London.

524 Crawley, M.J., 2013. The R Book, second ed. John Wiley and Sons, Chichester.

525 Danti, R., Della Rocca, G., Panconesi, A., 2013. Cypress canker, in: Gonthier, P.,
526 Nicolotti, G. (Eds.), Infectious Forest Diseases. CAB International, Wallingford, pp. 359–
527 375.

528 Dennert, F.G., Broggini, G.A., Gessler, C., Storari, M., 2015. *Gnomoniopsis castanea* is
529 the main agent of chestnut nut rot in Switzerland. Phytopathol. Mediterr. 54, 199–211.

530 Eckhardt, L.J., 2013. Blackstain root disease and other *Leptographium* diseases, in:
531 Gonthier, P., Nicolotti, G. (Eds.), Infectious Forest Diseases. CAB International,
532 Wallingford, pp. 283–296.

533 Edwards, A.M., 2008. Using likelihood to test for Lévy flight search patterns and for
534 general power-law distributions in nature. J. Anim. Ecol. 77, 1212–1222.

535 EFSA Panel on Plant Health (PLH), 2010. Risk assessment of the oriental chestnut gall
536 wasp, *Dryocosmus kuriphilus* for the EU territory on request from the European
537 commission. EFSA J. 8, 1619.

538 EPPO, 2005. Data sheets on quarantine pests – *Dryocosmus kuriphilus*. EPPO Bull. 35,
539 422–424.

540 Ferracini, C., Gonella, E., Ferrari, E., Saladini, M.A., Picciau, L., Tota, F., Pontini, M.,
541 Alma, A., 2015. Novel insight in the life cycle of *Torymus sinensis*, biocontrol agent of
542 the chestnut gall wasp. BioControl 60, 169–177.

543 Gardes, M., White, T.J., Fortin, A., Bruns, T.D., Taylor, J.W., 1991. Identification of
544 indigenous and introduced symbiotic fungi in ectomycorrhizae by amplification of
545 nuclear and mithocondrial ribosomal DNA. Can. J. Bot. 69, 180–190.

546 Gerber, H.U., Leung, B.P.K., Shiu, E.S.W., 2003. Indicator function and Hattendorff
547 theorem. N.A.A.J. 7, 38–47.

548 Giordano, L., Garbelotto, M., Nicolotti, G., Gonthier, P., 2013. Characterization of fungal
549 communities associated with the bark beetle *Ips typographus* varies depending on
550 detection method, location, and beetle population levels. Myc. Prog. 12, 127–140.

551 Gonthier, P., Lione, G., Giordano, L., Garbelotto, M., 2012. The American forest
552 pathogen *Heterobasidion irregulare* colonizes unexpected habitats after its introduction
553 in Italy. Ecol. Appl. 22, 2135–2143.

554 Griffiths, H.M., 2013. Forest diseases caused by prokaryotes: phytoplasmal and
555 bacterial diseases, in: Gonthier, P., Nicolotti, G. (Eds.), Infectious Forest Diseases. CAB
556 International, Wallingford, pp. 76–96.

557 Happ, G.M., Happ, C.M., Barras, S.J., 1971. Fine structure of the prothoracic
558 mycangium, a chamber for the culture of symbiotic fungi, in the southern pine beetle,
559 *Dendroctonus frontalis*. Tissue Cell 3, 295–308.

560 Harrington, T.C., 2013. *Ceratocystis* diseases, in: Gonthier, P., Nicolotti, G. (Eds.),
561 Infectious Forest Diseases. CAB International, Wallingford, pp. 230–255.

562 Harrison, M.D., Brewer, J.W., Merrill, L.D.,1980. Insect involvement in the transmission
563 of bacterial pathogens, in: Harris, K.F., Maramorosch, K. (Eds.), Vectors of Plant
564 Pathogens. Academic Press, New York, pp. 201–292.

565 Honkaniemi, J., Ojansuu, R., Piri, T., Kasanen, R., Lehtonen, M., Salminen, H.,
566 Kalliokoski, T., Mäkinen, H., 2014. Hmodel, a *Heterobasidion annosum* model for even-
567 aged Norway spruce stands. Can. J. Forest Res. 44, 796–809.

568 Jarnevich, C.S., Young, N., 2015. Using the MAXENT program for species distribution
569 modelling to assess invasion risk, in: Venette, R.C. (Ed.), Pest Risk Modelling and
570 Mapping for Invasive Alien Species. CAB International, Wallingford, pp. 65–81.

571 Jones, C.J., Lawton, J.H., Shachak, M., 1994. Organisms as ecosystem engineers.
572 Oikos 69, 373–386.

573 Jones, O., Maillardet, R., Robinson, A., 2009. Introduction to Scientific Programming
574 and Simulation Using R, CRC Press, Boca Raton.

Kato, K., Hijii, N., 1997. Effects of gall formation by *Dryocosmus kuriphilus* Yasumatsu (Hymenoptera: Cynipidae) on the growth of chestnut trees. J. Appl. Entomol. 121, 9–15.

Kendrick, B., 2000. The Fifth Kingdom, third ed. Mycologue Publications, Newburyport.

Kéry, M., 2010. Introduction to WinBUGS for Ecologists – A Bayesian Approach to Regression, ANOVA, Mixed Models and Related Analysis, Academic Press, London.

Kirisits, T., 2013. Dutch elm disease and other *Ophiostoma* diseases, in: Gonthier, P., Nicolotti, G. (Eds.), Infectious Forest Diseases. CAB International, Wallingford, pp. 256–281.

Lachene, B., 2013. On Pearson families of distributions and its applications. Afr. J. Math. Comput. Sci. Res. 6, 108–117.

Lione, G., Gonthier, P., 2016. A permutation-randomization approach to test the spatial distribution of plant diseases. Phytopathology 106, 19–28.

Lione, G., Giordano, L., Sillo, F., Gonthier, P., 2015. Testing and modelling the effects of climate on the incidence of the emergent nut rot agent of chestnut G*nomoniopsis castanea*. Plant Pathol. 64, 852–863.

Magro, P., Speranza, S., Stacchiotti, M., Martignoni, D., Paparatti, B., 2010. *Gnomoniopsis* associated with necrosis of leaves and chestnut galls induced by *Dryocosmus kuriphilus*. New Dis. Rep. 21, 15.

Maresi, G., Oliveira Longa, C.M., Turchetti, T., 2013. Brown rot on nuts of *Castanea sativa* Mill: an emerging disease and its causal agent. *i*Forest 6, 294–301.

595 Mitchell, A., 1999. The ESRI Guide to GIS Analysis – Volume 1: Geographic Patterns &
596 Relationships, ESRI Press, Redlands.

597 Mitchell, A., 2005. The ESRI Guide to GIS Analysis – Volume 2: Spatial Measurements
598 and Statistics, ESRI Press, Redlands.

599 Ôtake, A., 1980. Chestnut gall wasp, *Dryocosmus kuriphilus* Yasumatsu (Hymenoptera:
600 Cynipidae): a preliminary study on trend of adult emergence and some other ecological
601 aspects related to the final stage of its life cycle. Appl. Entomol. Zool. 15, 96-105.

602 Paine, T.D., Raffa, K.F., Harrington, T.C., 1997. Interactions among scolytid bark
603 beetles, their associated fungi, and live host conifers. Annu. Rev. Entomol. 42, 179–
604 206.

605 Pearson, K., 1895. Contributions to the mathematical theory of evolution, II: skew
606 variation in homogeneous material. Philos. Trans. Royal Soc. London 186, 343–414.

607 Petrini, O., 1991. Fungal endophytes of tree leaves, in: Andrews, J.H., Hirano, S.S.
608 (Eds.), Microbial Ecology of Leaves. Springer–Verlag, New York, pp. 179–197.

609 Quacchia, A., Moriya, S., Bosio, G., Scapin, I., Alma, A., 2008. Rearing, release and
610 settlement prospect in Italy of *Torymus sinensis*, the biological control agent of the
611 chestnut gall wasp *Dryocosmus kuriphilus*. BioControl 53, 829–839.

612 Redak, R.A., Purcell, A.H., Lopes, J.R.S., Blua, M.J., Mizell, R.F. III, Andersen, P.C.,
613 2004. The biology of xylem fluid-feeding insect vectors of *Xylella fastidiosa* and their
614 relation to disease epidemiology. Annu. Rev. Entomol. 49, 243–270.

615 Reynolds, A.M., Frye, M.A., 2007. Free-flight odor tracking in *Drosophila* is consistent
616 with an optimal intermittent scale-free search. PLoSONE 2, e354.

617 Sartor, C., Dini, F., Torello-Marinoni, D., Mellano, M.G., Beccaro, G.L., Alma, A.,
618 Quacchia, A., Botta, R., 2015. Impact of the Asian wasp *Dryocosmus kuriphilus*
619 (Yasumatsu) on cultivated chestnut: Yield loss and cultivar susceptibility. Sci. Hortic.
620 197, 454–460.

621 Sieber, T.C., Hugentobler, C., 1987. Endophytische Pilze in Blättern und Ästen
622 gesunder und geschädigter Buchen (*Fagus sylvatica* L.). Eur. J. For. Path. 6, 203–210.

623 Sillo, F., Giordano, L., Zampieri, E., Lione, G., De Cesare, S., Gonthier, P., 2016. HRM
624 analysis provides insights on the reproduction mode and the population structure of
625 *Gnomoniopsis castaneae* in Europe. Plant Pathol. DOI: 10.1111/ppa.12571

626 Somers, R.H., 1962. A new asymmetric measure of association for ordinal variables.
627 Am. Sociol. Rev. 27, 799–811.

628 Spence, N.J., 2001. Virus-vector interactions in plant virus disease transmission and
629 epidemiology, in: Jeger, M.J., Spence, N.J. (Eds.), Biotic Interactions in Plant-Pathogen
630 Associations. CABI Publishing, Wallingford, pp. 15–26.

631 Thébaud, G., Peyrard, N., Dallot, S., Calonnec, A., Labonne, G., 2005. Investigating
632 disease spread between two assessment dates with permutation tests on a lattice.
633 Phytopathology 95, 1453–1461.

634 Tamietti, G., 2016. On the fungal species *Gnomoniopsis castaneae* ("*castanea*") and its
635 synomym *G. smithogilvyi*. J. Plant Pathol. 98, 189–190.

636 Tilman, D., 1999. The ecological consequences of changes in biodiversity: a search for
637 general principles. Ecology 80, 1455–1474.

638 Venables, W.N., Ripley, B.D., 2002. Modern Applied Statistics with S, fourth ed.
639 Springer, New York.

640 Visentin, I., Gentile, S., Valentino, D., Gonthier, P., Tamietti, G., Cardinale, F., 2012.
641 *Gnomoniopsis castanea* sp. nov. (Gnomoniaceae, Diaporthales) as the causal agent of
642 nut rot in sweet chestnut. J. Plant Pathol. 94, 411–419.

643 Webber, J.F., 2004. Experimental studies on factors influencing the transmission of
644 Dutch elm disease. Investigación Agraria: Sistemas y Recursos Forestales 13, 197–
645 205.

646 White, T.J., Bruns, T., Lee, S.J.W.T., Taylor, J.W., 1990. Amplification and direct
647 sequencing of fungal ribosomal RNA genes for phylogenetics, in: Innis, M.A., Gelfand,
648 D.H., Sninsky, J.J., White, T.J. (Eds.), PCR Protocols: a Guide to Methods and
649 Applications. Academic Press, London, pp. 315–322.

650

Figure captions

Figure 1. Percentage of buds colonized by *Gnomoniopsis castaneae* (g_o) in the two samplings. The values of g_o observed in sampling 1 (white bars) and sampling 2 (gray bars) are reported separately for each site as well as conjointly for all the sites (i.e. Overall). Different letters on the top of the bars indicate a significant difference ($P<0.05$) between the g_o values of the two samplings according to the Fisher's exact test. Error bars refer to the 95% confidence interval of g_o.

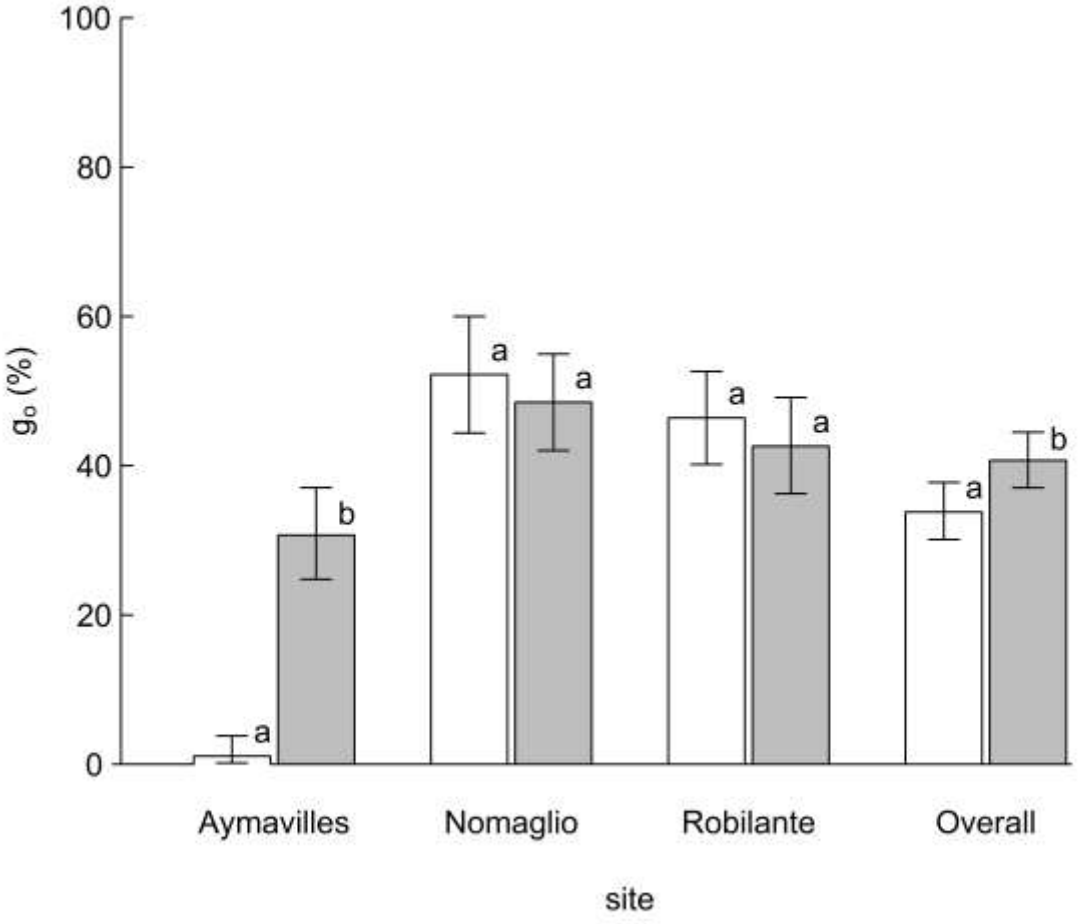

659 Table 1. Main characteristics of the sampling sites for the collection of buds and galls of *Dryocosmus kuriphilus* from the

660 European chestnuts.

site	coordinates (UTM WGS84 zone 32N)	elevation (m a.s.l)	aspect	No. of galls sampled	No. of buds sampled (20/06/2013)	No. of buds sampled (25/09/2013)
Aymavilles	361954, 5060322	980	W	175	186	225
Nomaglio	410670, 5043485	580	WSW	124	161	233
Robilante	381836, 4906525	730	WNW	24	250	230

661

662

663 Table 2. Negative binomial generalized linear regression models (nbGLM) comparing the average number of *Dryocosmus*
664 *kuriphilus* adults emerged from galls colonized (GC^+) and not colonized (GC^-) by *Gnomoniopsis castaneae*. The intercept,
665 the β coefficient and its related P-value are reported for each site and conjointly for all the sites (i.e. Overall). The β
666 coefficients showing a significant difference (P<0.05) between the averages are marked with the symbol *.

667

site	No. of *D. kuriphilus* adults emerged from GC^+ (average)	No. of *D. kuriphilus* adults emerged from GC^- (average)	intercept	β	P-value
Aymavilles	3.64	2.89	1.06	0.23*	$3.61 \cdot 10^{-2}$
Nomaglio	3.90	2.00	0.69	0.67*	$4.17 \cdot 10^{-7}$
Robilante	2.62	0.62	-0.47	1.43*	$1.88 \cdot 10^{-4}$
Overall	3.76	2.54	0.93	0.39*	$5.88 \cdot 10^{-9}$

668

669

Table 3. Blocks of Monte Carlo simulations defined by the combination of *Gnomoniopsis castaneae* colonization (g) and *Dryocosmus kuriphilus* oviposition (d). The average of the odds ratios $\bar{\theta}$, along with its 95% CI lower and upper bounds ($\bar{\theta}_l$, $\bar{\theta}_u$), are reported for each g-d combination and hypothesis within scenario as measures of association between fungal colonization and oviposition.

block		scenario A		scenario B	
g	d	hypothesis A_1	hypothesis A_2	hypothesis B_1	hypothesis B_2
20	20	1.14 (0.17, 3.00)	15.65 (3.70, 50.00)	1.13 (0.18, 2.95)	6.00 (1.68, 15.96)
20	40	0.97 (0.00, 2.60)	20.55 (5.45, 60.57)	1.13 (0.30, 2.90)	5.74 (1.79, 15.44)
20	60	1.14 (0.35, 2.64)	32.05 (7.50, 100.00)	1.13 (0.34, 2.76)	6.00 (1.68, 17.83)
20	80	0.25 (0.00, 1.82)	35.47 (8.00, 85.00)	1.16 (0.38, 2.91)	6.25 (1.60, 22.97)
40	20	1.14 (0.34, 2.75)	15.70 (3.80, 42.16)	1.13 (0.32, 2.68)	9.78 (2.64, 41.17)
40	40	0.93 (0.00, 2.20)	18.35 (5.21, 57.79)	1.08 (0.41, 2.29)	7.18 (2.66, 16.57)
40	60	1.08 (0.44, 2.20)	21.61 (6.91, 56.36)	1.07 (0.44, 2.21)	6.61 (2.54, 15.44)
40	80	0.16 (0.00, 1.48)	26.22 (8.50, 70.30)	1.10 (0.45, 2.25)	6.41 (2.39, 15.28)
50	60	0.15 (0.00, 1.54)	22.61 (6.67, 69.21)	1.08 (0.46, 2.21)	7.81 (3.05, 17.90)

60	20	1.20 (0.36, 2.97)	10.75 (3.23, 17.70)	1.16 (0.37, 2.88)	12.57 (3.38, 21.53)
60	40	0.96 (0.00, 2.28)	17.48 (4.73, 41.13)	1.11 (0.46, 2.34)	13.83 (3.74, 52.04)
60	60	1.10 (0.46, 2.25)	22.61 (5.86, 71.30)	1.09 (0.46, 2.20)	10.75 (3.64, 29.06)
60	80	0.16 (0.00, 1.47)	26.17 (6.91, 102.50)	1.07 (0.46, 2.14)	8.75 (3.32, 19.78)
80	20	1.39 (0.30, 5.45)	4.78 (2.24, 6.25)	1.35 (0.34, 5.68)	6.58 (3.08, 7.90)
80	40	1.22 (0.37, 3.33)	9.80 (3.51, 14.29)	1.20 (0.40, 2.96)	14.49 (4.83, 20.24)
80	60	0.13 (0.00, 1.48)	9.52 (3.30, 14.05)	1.14 (0.40, 2.57)	20.83 (5.44, 38.84)
80	80	0.15 (0.00, 1.54)	19.37 (5.47, 40.00)	1.13 (0.39, 2.51)	21.86 (5.25, 60.80)

675

676

677